that considerable multiple-bond character between the rhenium atoms is maintained in these mixed-metal cluster compounds. This is further supported by the fact that the ESR spectrum of $[Au_2Re_2(H)_6(PPh_3)_6]^+$ (**1**), with respect to g value and hyperfine coupling constants, is somewhat similar to that of the oxidized parent complex prepared by Walton.[36]

Comparison of the present work to the work of Caulton[26] and Walton[27] leads us to conclude that the starting gold(I) phosphine complex significantly affects the course of the reaction and determines the final product(s). If an acidic anion is used, then the fully protonated Au_2Re_2 cluster $[Au_2Re_2(H)_8(PPh_3)_6]^{2+}$ (**4**) is formed.[27] The use of counterions of varying basicity leads to clusters $Au_2Re_2(H)_6(PPh_3)_6$ (**3**) or $[Au_2Re_2(H)_7(PPh_3)_6]^+$ (**5**), in which all[26] or some of the hydride ligands with acidic character have been abstracted. This work shows the noninnocence of the NO_3^- ion in the formation of these gold–rhenium clusters. When present in a reaction mixture where H^+ is being generated, the NO_3^- ion can oxidize the clusters with accessible oxidation potentials.

Acknowledgment. This work was supported by the National Science Foundation (Grant CHE-851923) and the donors of the Petroleum Research Fund, administered by the American Chemical Society. We gratefully acknowledge the Johnson Matthey Co. for a generous loan of gold salts.

Registry No. **1**(PF_6), 107712-43-6; **2**$(PF_6)_2$, 117226-13-8; **3a**, 117201-64-6; **3b**, 117201-65-7; **4**$(BF_4)_2$, 117201-66-8; **5**(BF_4), 117201-67-9; $[(Ph_3PAu)_3O]BF_4$, 53317-87-6; K(O-*t*-Bu), 865-47-4; $[Fe(C_5H_5)_2]PF_6$, 11077-24-0; $Re_2(H)_8(PPh_3)_4$, 66984-37-0; Re, 7440-15-5; Au, 7440-57-5; sodium naphthalenide, 3481-12-7.

Supplementary Material Available: Figures of cyclic voltammetric and spectroelectrochemical experiments on $[Au_2Re_2(H)_7(PPh_3)_6]^+$ (2 pages). Ordering information is given on any current masthead page.

Contribution from the Istituto per lo Studio della Stereochimica ed Energetica dei Composti di Coordinazione, CNR, Via J. Nardi 39, 50132 Florence, Italy, Dipartimento di Chimica dell'Università di Siena, 53100 Siena, Italy, and Departamento de Quimica, Universidad de Valencia, Valencia, Spain

Synthesis, Characterization, and Electrochemical Properties of a Family of Dinuclear Rhodium Complexes Containing Two Terminal Hydride Ligands and Two Hydride (or Chloride) Bridges. Stoichiometric and Catalytic Hydrogenation Reactions of Alkynes and Alkenes

Claudio Bianchini,*[,1] Andrea Meli,[1] Franco Laschi,[2] José A. Ramirez,[3] Piero Zanello,[2] and Alberto Vacca[1]

Received March 31, 1988

Protonation by strong acids and thermal decomposition in solution are two routes by which the trihydride (triphos)RhH_3 (**1**) [triphos = $MeC(CH_2PPh_2)_3$] is used to synthesize the tetrahydrido complexes $[(triphos)RhH(\mu\text{-}H)_2HRh(triphos)](BPh_4)_2$ (**2**) and $[(triphos)RhH(\mu\text{-}H)_2HRh(triphos)]$ (**3**), respectively. The bis(μ-chloro) dihydride $[(triphos)RhH(\mu\text{-}Cl)_2HRh(triphos)](BPh_4)_2$ (**6**) can be prepared either by protonation of (triphos)$RhCl(C_2H_4)$ followed by $NaBPh_4$ addition or by H/Cl exchange between **2** and CH_2Cl_2. Interestingly, **6** exists in solution as a 1:1 mixture of two geometric isomers. The electrochemical behavior of the tetrahydride derivatives in nonaqueous solvents shows that they can reversibly undergo one-electron-redox changes with no change of the primary geometry. By contrast, **6** is unable to reversibly accept or lose electrons. Electrochemical techniques have been used to generate the paramagnetic $[(triphos)RhH(\mu\text{-}H)_2HRh(triphos)]^+$ derivative, which is not directly obtainable by chemical methods. All of the compounds have been fully characterized by IR, NMR, and ESR techniques. Both the mononuclear trihydride **1** and the dimeric tetrahydride **2** are able to straightforwardly transfer hydrogen atoms to unsaturated substrates such as 3,3-dimethylbut-1-ene, dimethyl maleate (DMMA), or dimethyl acetylenedicarboxylate (DMAD). The effectiveness of **2** and **6** to catalytically hydrogenate DMAD and DMMA is investigated and compared to that shown by the mononuclear species $[(triphos)Rh(\pi\text{-}DMAD)]BPh_4$ and $[(triphos)Rh(\pi\text{-}DMMA)]BPh_4$ as well as a family of homo- and heterobimetallic $(\mu\text{-}H)_3$ complexes of formula $[(triphos)Rh(\mu\text{-}H)_3M(triphos)]^{n+}$ (M = Rh, Co; n = 3, 2). All of the compounds prove active catalysts or catalyst precursors for hydrogenation reactions of DMAD and DMMA. The catalyzed alkyne hydrogenation yields largely the olefin. In the catalytic cycles some of the binuclear compounds are resistant to fragmentation and are responsible for the catalysis.

Introduction

Polynuclear polyhydrides[4] are of interest because of their effective role in homogeneous catalytic hydrogenations and their ability to model surface chemistry.[5] A perusal of the large body of experimental information on polynuclear polyhydrides reveals the paucity of electrochemical data on these compounds[6] as well

(1) CNR.
(2) Università di Siena.
(3) Universidad de Valencia.
(4) (a) Moore, D. R.; Robinson, S. D. *Chem. Soc. Rev.* **1983**, *12*, 415. (b) Hlatky, G. G.; Crabtree, R. H. *Coord. Chem. Rev.* **1985**, *65*, 1. (c) Soloveichik, G. L.; Bulydev, B. M. *Russ. Chem. Rev.* **1982**, *51*, 286. (d) Bau, R.; Carroll, W. E.; Hart, D. W.; Teller, R. G.; Koetzle, T. F. In *Transition Metal Hydrides*; Bau, R., Ed.; Advances in Chemistry 167; American Chemical Society: Washington, DC, 1978; p 73.
(5) (a) Parshall, G. W. *Homogeneous Catalysis*; Wiley-Interscience: New York, 1980. (b) James, B. R. *Homogeneous Hydrogenation*; Wiley-Interscience: New York, 1973. (c) Maitlis, P. M. *Acc. Chem. Res.* **1978**, *11*, 301. (d) Sivak, A. J.; Muetterties, E. L. *J. Am. Chem. Soc.* **1979**, *101*, 4878. (e) Crabtree, R. H; Felkin, H.; Morris, G. E. *J. Organomet. Chem.* **1977**, *141*, 205. (f) Burch, R. R.; Muetterties, E. L.; Day, V. W. *Organometallics* **1982**, *1*, 186. (g) Chaudret, B.; Devillers, J.; Poilblanc, R. *Ibid.* **1985**, *4*, 1727. (h) Wang, H.-H.; Casalnuovo, A. L.; Johnson, B. J.; Mueting, A. M.; Pignolet, L. H. *Inorg. Chem.* **1988**, *27*, 325.

0020-1669/88/1327-4429$01.50/0

Scheme I

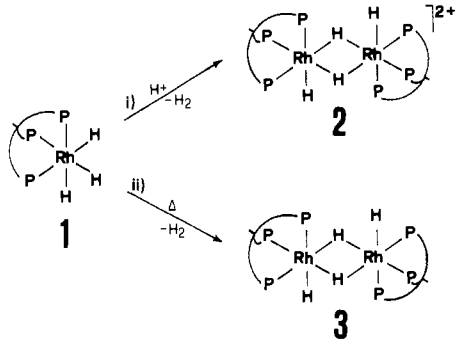

as the scarcity of systematic comparisons of the catalytic activity of polymetallic species vs related mononuclear complexes. It is with the synthesis, characterization, and electrochemistry of a family of polyhydrido dirhodium complexes and with their hydrogenation reactions of dimethyl maleate (DMMA) and dimethyl acetylenedicarboxylate (DMAD) that the present paper is largely concerned. We also compare the catalytic activity of bimetallic species with that of related mononuclear complexes.

A preliminary account of part of this work has already appeared.[7]

Results

Dihydrido-Bridged Complexes. In addition to the donor–acceptor reaction pathway recently reported by us[6c] and other authors,[8] the trihydride (triphos)RhH_3 (**1**)[9] can function as precursor to polynuclear polyhydride derivatives by two additional routes, namely (i) protonation by strong acids, followed by $NaBPh_4$ addition and (ii) thermal decomposition in THF (Scheme I).

In both cases, the system evolves H_2 through reductive elimination reactions. The yellow orange, terminal-bridged tetrahydrido complex [(triphos)$RhH(\mu\text{-}H)_2HRh$(triphos)]$(BPh_4)_2$ (**2**) is obtained by treatment of **1** in CH_2Cl_2 or THF with $HOSO_3CF_3$, followed by addition of $NaBPh_4$ in ethanol. Compound **2** is diamagnetic, quite stable in the solid state and in deoxygenated DMF, CH_2Cl_2, and $EtNO_2$ solutions in which it behaves as a 1:2 electrolyte. The presence of terminal hydride ligands is evidenced by a strong IR absorption at 1980 cm^{-1}. The compound is stereochemically nonrigid in solution; the bridged–terminal interconversion of the four hydride ligands is rapid on the NMR time scale to −60 °C so that each hydrogen atom appears magnetically equivalent with all rhodium and phosphorus atoms. As a matter of fact, the ^1H NMR spectrum (CD_2Cl_2) in the hydridic hydrogen region exhibits an unresolved multiplet at δ −10.6 (4 H) also at low temperature, and the $^{31}P\{^1H\}$ NMR (DMF, 203 K) spectrum consists of a broad doublet centered at 25.24 ppm (J_{PRh} = 90 Hz).

A dimeric complex strictly related to **2** is the neutral product obtained by refluxing **1** in THF (Scheme I). The liver red complex, of formula [(triphos)$RhH(\mu\text{-}H)_2HRh$(triphos)] (**3**), is diamagnetic and very poorly soluble in common organic solvents so as to preclude a meaningful characterization by spectroscopic techniques. The IR spectrum (Nujol mulls) exhibits a strong ν(Rh–H) vibration at 1960 cm^{-1}. There is no doubt that **2** and **3** form a two-electron redox couple as demonstrated by electrochemical and chemical investigations.

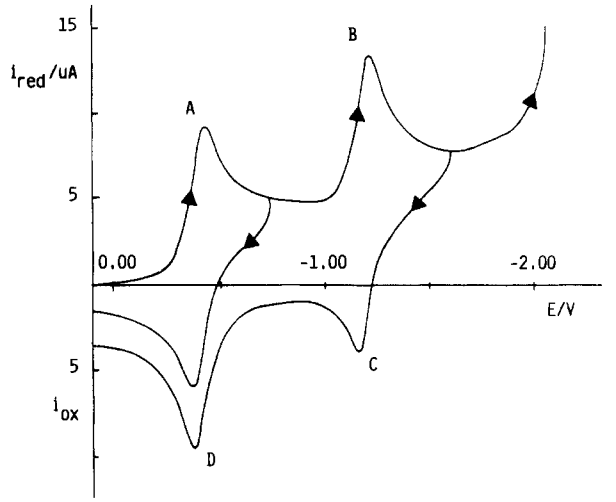

Figure 1. Cyclic voltammogram recorded at a platinum electrode on a MeCN solution containing **2** (5.0×10^{-4} mol cm^{-3}) and $[NEt_4]ClO_4$ (0.1 mol dm^{-3}). Scan rate: 0.2 V s^{-1}.

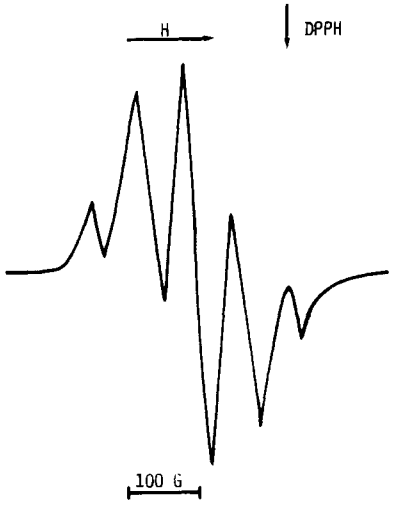

Figure 2. X-Band ESR spectrum at 300 K of electrogenerated [(triphos)$RhH(\mu\text{-}H)_2HRh$(triphos)]$^+$ in MeCN.

Figure 1 reports the cyclic voltammetric response exhibited by **2** in deaerated MeCN solution. Two successive reduction processes are displayed (peaks A and B), each of which shows a directly associated reoxidation response in the reverse scan (peaks D and C, respectively). Controlled-potential coulometric tests reveal that each step involves a one-electron process. Analysis[10] of the cyclic voltammetric peak system A/D with scan rates, v, varying from 0.02 to 50 V s^{-1} shows that (i) the i_{pa}/i_{pc} ratio is constantly equal to unity, (ii) the $i_{pc}v^{-1/2}$ term is constant, and (iii) the difference $E_{pa} - E_{pc} = \Delta E_p$ is equal to 60 mV up to 2 V s^{-1}, then gradually increases up to 150 mV at 50 V s^{-1}, which is likely due to some uncompensated solution resistances. The same features are displayed by the second reduction process. These data indicate that the redox activity of the complex cation $[RhH(\mu\text{-}H)_2HRh]^{2+}$ is consistent with the two uncomplicated one-electron reduction steps:

$$[RhH(\mu\text{-}H)_2HRh]^{2+} \underset{-e^-}{\overset{+e^-}{\rightleftharpoons}} [RhH(\mu\text{-}H)_2HRh]^{+} \qquad E^{\circ\prime} = -0.42 \text{ V}$$

$$[RhH(\mu\text{-}H)_2HRh]^{+} \underset{-e^-}{\overset{+e^-}{\rightleftharpoons}} [RhH(\mu\text{-}H)_2HRh] \qquad E^{\circ\prime} = -1.19 \text{ V}$$

(6) (a) Allison, J. D.; Walton, A. *J. Am. Chem. Soc.* **1984**, *106*, 163. (b) Moehring, G. A.; Walton, R. A. *J. Chem. Soc., Dalton Trans.* **1987**, 715. (c) Bianchini, C.; Meli, A.; Zanello, P. *J. Chem. Soc., Chem. Commun.* **1986**, 628. (d) Klingher, R. J.; Huffman, J. C.; Kochi, J. K. *J. Am. Chem. Soc.* **1980**, *102*, 208.

(7) Bianchini, C.; Mealli, C.; Meli, A.; Sabat, M. *J. Chem. Soc., Chem. Commun.* **1986**, 777.

(8) (a) Rhodes, L. F.; Huffman, J. C.; Caulton, K. G. *J. Am. Chem. Soc.* **1983**, *105*, 5137. (b) Rhodes, L. F.; Huffman, J. C.; Caulton, K. G. *Ibid.* **1984**, *106*, 6874. (c) Rhodes, L. F.; Huffman, J. C.% Caulton, K. G. *Ibid.* **1985**, *107*, 1759. (d) Lehner, H.; Matt, D.; Togni, A.; Thouvenot, R.; Venanzi, L. M.; Albinati, A. *Inorg. Chem.* **1984**, *23*, 4254. (e) Albinati, A.; Lehner, H.; Venanzi, L. M. *Ibid.* **1985**, *24*, 1483. (f) Geerts, R. F.; Huffman, J. C.; Caulton, K. G. *Ibid.* **1986**, *25*, 590. (g) Albinati, A.; Emge, T. J.; Koetzle, T. F.; Meille, S. V.; Musco, A.; Venanzi, L. M. *Ibid.* **1986**, *25*, 4821. (h) Lemmen, T. H.; Huffman, J. C.; Caulton, K. G. *Angew. Chem., Int. Ed. Engl.* **1986**, *25*, 262. (i) Abrahams, S. C.; Ginsberg, A. P.; Koetzle, T. T.; Marsch, P.; Sprinkle, C. R. *Inorg. Chem.* **1986**, *25*, 2500.

(9) Ott, J.; Venanzi, L. M.; Ghilardi, C. A.; Midollini, S.; Orlandini, A. *J. Organomet. Chem.* **1985**, *291*, 89.

(10) Brown, E. R.; Sandifer, J. R. In *Physical Methods of Chemistry. Electrochemical Methods*; Rossiter, B. W., Hamilton, J. F., Eds.; Wiley: New York, 1986; Vol. 2, Chapter 4.

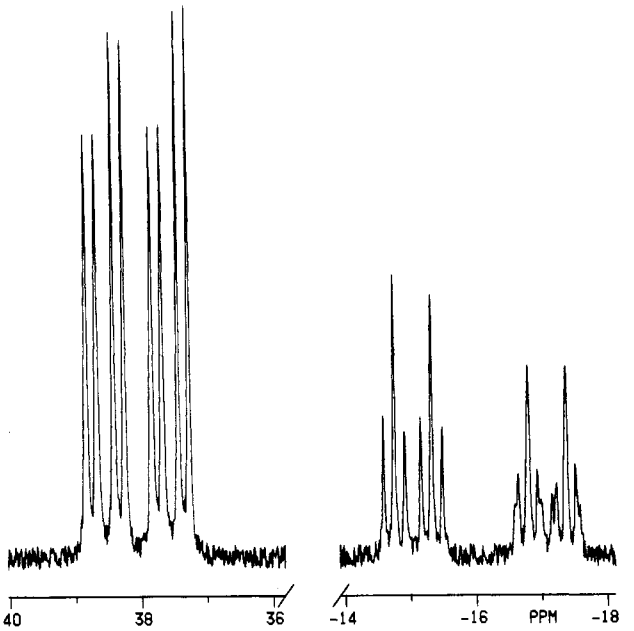

Figure 3. $^{31}P\{^1H\}$ NMR spectrum of **6** (298 K, nitromethane, 121.42 MHz, 85% H_3PO_4 reference).

The electrochemical reversibility of these redox changes suggests that no significant structural reorganization within the complex framework occurs as a consequence of the addition or removal of electrons. As expected, a sample of **3** prepared according to Scheme I gives rise in cyclic voltammetry to two distinct one-electron oxidation steps at the same potentials of the couples $[RhH(\mu\text{-}H)_2HRh]/[RhH(\mu\text{-}H)_2HRh]^+$ and $[RhH(\mu\text{-}H)_2HRh]^+/[RhH(\mu\text{-}H)_2HRh]^{2+}$, respectively.

The X-band ESR spectrum of the paramagnetic cation $[(triphos)RhH(\mu\text{-}H)_2HRh(triphos)]^+$ electrogenerated by macroelectrolysis at −0.7 V, is reported in Figure 2. The spectrum (MeCN, 300 K) exhibits a well-resolved quintuplet ($\langle g \rangle$ = 2.083) consistent with strong coupling of one unpaired electron to four equivalent phosphorus nuclei as indicated by the hyperfine coupling constant of 70.3 G.[11] Four equivalent phosphorus atoms can be easily found in a structure in which two octahedral rhodium centers are joined through a common edge defined by two bridging hydride ligands. On the other hand, such a primary structure for dimeric rhodium complexes of general formula $(triphos)RhH(\mu\text{-}Y)_2HRh(triphos)$ is well established.[12] In addition, the $P_2Rh(\mu\text{-}Y)_2RhP_2$ fragment is generally planar and permits extensive electronic delocalization.[11a] The line shape of the spectrum does not evidence any additional hyperfine structure, probably on account of small coupling of the electron to rhodium and the residual phosphorus nuclei. In this respect, notice that the line width of the five absorptions is relatively large, the narrowest one being 32 G.

Unfortunately, all our attempts to isolate the monocationic derivative in the solid state were unsuccessful, due to its extreme sensitivity to oxygen. Actually, every attempt to work up the orange brown solution of the electrogenerated monocationic derivative led to the obtainment of the oxidized species **2**.

In nice agreement with the electrode potentials, the complex cation $[(triphos)RhH(\mu\text{-}H)_2HRh(triphos)]^+$ forms as determined by ESR spectroscopy, by mixing equimolar MeCN solutions of **2** and **3**.

Dichloro-Bridged Complexes. When the protonation of **1** is carried out in CH_2Cl_2 and the dimeric product **2** is not immediately precipitated but left standing in the reaction mixture for 2–3 h, the crude crystalline crop obtained by $NaBPh_4$ addition contains

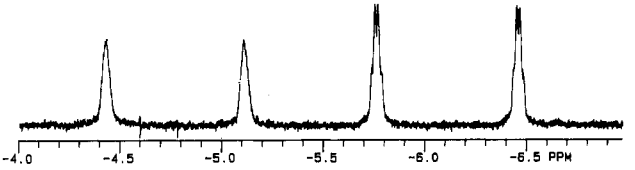

Figure 4. ^1H NMR spectrum of **6** (CD_2Cl_2, 293 K, 300 MHz, Me_4Si reference) (hydride region).

side products in variable yields (10–20% over several preparations). Such impurities give rise to two noninteracting $^{31}P\{^1H\}$ NMR AM_2X spin systems, one of the two being somewhat complicated in the A portion. The same AM_2X spin systems are observed as a function of time in CH_2Cl_2 solutions of **2**, i.e. the longer **2** is maintained in solution, the higher is the amount of these additional resonances as monitored by NMR spectroscopy. We have found that protonation of the Rh(I) complex $(triphos)RhCl(C_2H_4)$ (**5**),[7] in CH_2Cl_2 by $HOSO_3CF_3$, followed by $NaBPh_4$ addition in ethanol gives pink crystals. The $^{31}P\{^1H\}$ NMR spectrum of this compound in nitromethane (Figure 3) exactly coincides with that of the side products, which form upon dissolution of **2** in CH_2Cl_2.

The pink crystals are quite stable in the solid state and in deaerated solutions in which they behave as a 1:2 electrolyte. The IR spectrum both in the solid state and in solution exhibits a medium-intensity absorption at 2020 cm^{-1} that is attributable to a Rh–H(terminal) stretching vibration. On the basis of all of these data as well as molecular weight and microanalytical measurements, the product is assigned the dimeric formulation $[(triphos)RhH(\mu\text{-}Cl)_2HRh(triphos)](BPh_4)_2$ (**6**). However, there is no doubt that the compound exists, at least in solution, as a 1:1 mixture of two isomeric forms.[13] This can be also deduced by the ^1H NMR spectrum (CD_2Cl_2, 293 K) shown in Figure 4, which shows the presence of two different couples of hydride ligands.

A perusal of the possible conformations that a compound such as **6** may adopt limits to two the number of isomers, namely *trans*-**6** and *cis*-**6**, where trans and cis refer to the mutual disposition of the terminal hydride ligands.

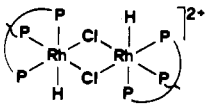

trans-**6**

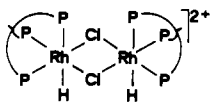

cis-**6**

Interestingly, the two isomers form in a 1:1 ratio regardless of the synthetic procedure. This fact and the absence of any fluxionality on the NMR time scale, even at high temperatures (up to 60 °C), indicate that the interconversion, if any, between *trans*-**6** and *cis*-**6** is rather slow. Heating of the solution above 60 °C results in the decomposition of both species, whereas at low temperatures both the proton and phosphorus NMR spectra do not significantly change. Unfortunately, all our attempts to separate the two compounds as well as to grow crystals suitable for an X-ray analysis were unsuccessful. Accordingly, it is not possible at this stage to precisely correlate structures and NMR patterns. Tentatively, we suggest that the hydridic resonance at higher field belongs to the trans isomer. In fact, it is reasonable to assign the first-order doublet of quartets (AMQ_2X spin system) at δ −6.12 ($J_{HPtrans}$ = 209.8 Hz, J_{HPcis} = 5.3 Hz, J_{HRh} = 4.4 Hz) to the hydride ligands in the more symmetrical trans conformation. In turn, the poor resolution of the doublet of multiplets at δ −4.77 ($J_{HPtrans}$ = 201.5 Hz) may be due to second-order effects originated by the probable magnetic nonequivalence of the two hydride ligands in the cis isomer. As a matter of fact, a splitting pattern of the type $[AMQ_2X]_2$ computed by using the J_{AQ} and J_{AX} values measured for the trans isomer and introducing $J_{AM} = J_{A'M'}$ = 201.5 Hz and $J_{AA'} = \simeq 5$ Hz well reproduces the experimental line shape

(11) (a) Bianchini, C.; Meli, A.; Laschi, F.; Vacca, A.; Zanello, P. *J. Am. Chem. Soc.* **1988**, *110*, 3913. (b) Pilloni, G.; Zotti, G.; Zecchini, S. *J. Organomet. Chem.* **1986**, *317*, 357.

(12) Bianchini, C.; Mealli, C.; Meli, A.; Sabat, M. *Inorg. Chem.* **1986**, *25*, 4617.

(13) A dimeric rhodium complex showing ^1H and ^{31}P NMR spectra quite similar to those of **2** is reported in ref 15. The compound was prepared by reaction of $[(triphos)RhCl_3]$ with H_2 in MeOH and isolated as the BF_4^- salt. Also in that case, a 1:1 mixture of two isomeric products was postulated: L. Venanzi, ETH Zürich, private communication.

Scheme II

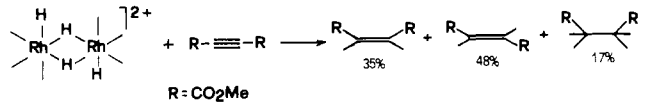

Table I. Results of Catalytic Hydrogenations of DMAD[a] at 1 atm of Hydrogen Pressure in DMF

catalyst	T, °C	% conversion	% composition of products DMMA	DMFU	DMSU	rate[b]
$[RhH(\mu\text{-}H)_2HRh]^{2+}$	80	50	91.9	1.1	7.0	
		100	88.7	2.1	9.2	31.3
	25	17.1[c]	65.8	19.9	14.3	1.4
$[RhH(\mu\text{-}Cl)_2HRh]^{2+}$	80	50	90.4	5.3	4.3	
		100	86.0	7.5	6.5	29.8
	25	4.1[c]	61.2	22.4	16.4	0.3
$[Rh(\mu\text{-}H)_3Rh]^{2+}$	80	50	91.6	2.6	5.8	
		100	88.3	3.3	8.4	19.1
	25	3.3[c]	64.3	31.3	4.6	0.2
$[Rh(\mu\text{-}H)_3Co]^{2+}$	80	50	96.3	0.5	3.2	
		100	92.1	1.6	6.3	13.7
	25	11.7[c]	65.8	20.5	13.7	0.9
$[Rh(\mu\text{-}H)_3Rh]^{3+}$	80	50	92.1	1.7	6.2	
		100	87.5	1.9	10.6	60.6
	25	10.2[c]	68.4	18.4	13.2	0.8
$[Rh(DMAD)]^{+}$	80	50	84.1	5.8	10.1	
		100	81.5	7.2	11.3	77.2
	25	29.5[c]	46.1	14.6	39.3	1.6

[a] DMAD to metal mole ratio of 30:1. [b] Rate reported as moles of DMMA per mole of metal per hour. [c] Values after 150 min.

of the hydride ligands in the cis isomer. Obviously, such a treatment is far from being rigorous and serves only to qualitatively confirm our assumption.

For a similar argument, the AM_2X spin system in which the A portion is evidently first order is assigned to the trans isomer. Accordingly, we propose the following ^{31}P NMR assignments: *trans*-**6** δ(A) − 15.04 ppm, dt, J_{AM} = 19.8 Hz, J_{ARh} = 69.4 Hz, δ(M) 37.83 ppm, dd, J_{MRh} = 118.9 Hz; *cis*-**6** δ(A) −17.08 ppm, dt, J_{AM} = 19.9 Hz, J_{ARh} = 70.2 Hz, δ(M) 38.25 ppm, dd, J_{MRh} = 120.9 Hz. Due to the poor resolution of the experimental spectrum, it was not possible to determine the other couplings that are responsible for the evident second-order effects (see Figure 3).

Hydrogen-Transfer Reactions. The effectiveness **2** and **6** to hydrogenate dimethyl acetylenedicarboxylate (DMAD) and dimethyl maleate (DMMA) has been investigated and compared with that shown by the two mononuclear complexes [(triphos)Rh(π-DMAD)]BPh_4 (**7**)[14] and [(triphos)Rh(π-DMMA)]BPh_4 (**8**),[14] as well as the $(\mu\text{-}H)_3$ homo- or heterobinuclear complexes [(triphos)Rh(μ-$H)_3$Rh(triphos)]$(BPh_4)_2$ (**9**), [(triphos)Rh(μ-$H)_3$Rh(triphos)]$(BF_4)_3$ (**10**), and [(triphos)Rh(μ-$H)_3$Co(triphos)]$(ClO_4)_2$ (**11**).[6c] The experimental conditions used are described in the Experimental Section. The hydrogenation of DMAD and DMMA proved convenient for GC purposes.

Hydrogenation of DMAD. The only complex within the present series of polyhydrido complexes that is able by itself to effectively transfer hydrogen atoms to DMAD is the tetrahydride **2**. Stirring DMAD (2 mmol) with **2** (1 mmol) in DMF at room temperature for 8 h results in hydrogenation of the carbon–carbon triple bond and, as the predominant reaction, produces DMMA and its trans isomer dimethyl fumarate (DMFU). An appreciable amount of dimethyl succinate (DMSU) is also found in (Scheme II).

At the end of the reaction the originarily yellow-orange solution **2** is completely colorless and, by addition of *n*-heptane, separates a rhodium/triphos-containing product whose chemical composition is still unknown.

By contrast, at 1 atm of H_2, all of the compounds in DMF solutions at 22 °C catalyze, although very slowly, the hydrogenation of DMAD to DMMA, DMFU, and DMSU (Table I). The total amount of alkane and isomerized olefin is generally smaller than that of the cis olefin, thus indicating that the alkene competes but does not prevail over the alkyne for coordination sites on the catalyst precursors or intermediates. In contrast, with the mononuclear complex **7**, DMSU and DMFU constitute 54% of the products showing that the cis olefin is bound to the metal center much stronger than in the dimeric complexes.

Table II. Results of Catalytic Hydrogenations of DMMA[a] at 1 atm of Hydrogen Pressure in DMF

catalyst	T, °C	% conversion	% composition of products DMSU	DMFU	rate[b]
$[RhH(\mu\text{-}H)_2HRh]^{2+}$	80	50	87.3	12.7	
		100	88.4	11.6	
		100	100		24.3
	25	44.7[c]	67.1	32.9	1.5
$[RhH(\mu\text{-}Cl)_2HRh]^{2+}$	80	50	100		
		100	99.3	0.7	
		100	100		21.7
	25	3.4[c]	64.2	35.8	0.1
$[Rh(\mu\text{-}H)_3Rh]^{2+}$	80	50	59.8	40.2	
		100	90.4	9.6	
		100	100		15.7
	25	40.9[c]	75.5	24.5	1.5
$[Rh(\mu\text{-}H)_3Co]^{2+}$	80	50	65.9	34.1	
		100	90.4	9.6	
		100	100		5.5
	25	4.2[c]	73.2	26.8	0.1
$[Rh(\mu\text{-}H)_3Rh]^{3+}$	80	50	86.8	13.2	
		100	95.8	4.2	
		100	100		24.7
	25	3.8[c]	73.8	26.2	0.1
$[Rh(DMMA)]^{+}$	80	50	95.5	4.5	
		100	97.8	2.2	
		100	100		45.0
	25	18.4[c]	100		0.9

[a] DMMA to metal mole ratio of 30:1. [b] Rate reported as moles of DMSU per mole of metal per hour. [c] Values after 360 min.

At 80 °C, the hydrogenation of DMAD proceeds much faster and the selectivity in the cis olefin increases (see Table I). This clearly indicates that at high temperature the coordinated olefin is easily displaced by the alkyne before it can isomerize or be hydrogenated to alkane. The effectiveness of the complexes to act as hydrogenation catalysts toward DMAD at 80 °C in DMF (100% conversion) is in the following order:

$$[Rh(\pi\text{-DMAD})]^{+} > [Rh(\mu\text{-}H)_3Rh]^{3+} > [RhH(\mu\text{-}H)_2HRh]^{2+} > [RhH(\mu\text{-}Cl)_2HRh]^{2+} > [Rh(\mu\text{-}H)_3Rh]^{2+} > [Rh(\mu\text{-}H)_3Co]^{2+}$$

The turnover rate, which is reported as moles of product per mole of metal per hour, shows that the mononuclear species is more active than the dimeric ones, both at room temperature and high temperature, therefore showing that eventual cooperative effects which may result from the presence of two metals do not positively influence the reaction rate. However, for mechanisms involving distinct roles for the two metals (see below), the rates calculted as moles of product per mole of complex are essentially comparable. Interestingly, the mononuclear complex is less selective than the dimers in the hydrogenation of the triple bond.

The fate and the rate of disappearance of DMMA and DMFU are almost identical with results described in the next section.

Hydrogenation of DMMA. The tetrahydride **2** (DMF, at room temperature) quantitatively hydrogenates in 8 h DMMA to DMSU. When an excess of the olefin is used, isomerization is observed with a stoichiometry of one DMFU per molecule of dimer. At 80 °C in DMF, the ratio increases up to 4. Under the same reaction conditions all of the other compounds are quite inactive toward DMMA. By contrast, at 1 atm of hydrogen pressure in DMF, they prove active catalysts for the hydrogenation of DMMA. As in the case of DMAD, the reaction rates increase on increasing the temperature (Table II). The activity at 80 °C is in the same order as that found for the hydrogenation of DMAD although the rates are lower.

(14) Bianchini, C.; Meli, A., manuscript in preparation.
(15) Ott, J. Dissertation, ETH No. 8000, Zürich, Switzerland, 1986.

Scheme III

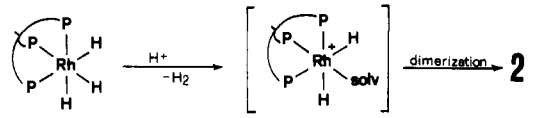

Scheme IV

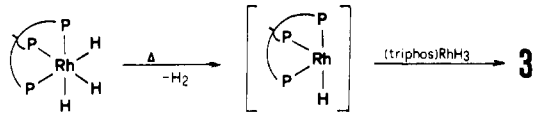

Scheme V

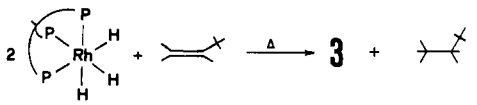

The hydrogenation reactions are generally accompanied by competing olefin isomerization. In particular, the $[Rh(\mu\text{-}H)_3Rh]^{2+}$ dimer exhibits nearly equal initial rates of hydrogenation and isomerization (see the values at 50% conversion).

Invariably, the hydrogenation of the isomerization product, DMFU, occurs after that of DMMA and at lower rate. As in the case of DMAD, the reactions proceed without disturbing the CO_2Me groups.

Discussion

Dihydro-Bridged Complexes. Although through different intermediates, the reactions leading to **2** and **3** (Scheme I) appear mechanistically very similar. In both cases, in fact, it is reasonable to think of the preliminary formation of coordinatively and electronically unsaturated mononuclear species that are stabilized by dimerization. In particular, protonation of **1** most likely involves the formation of a rhodium(V) tetrahydride. Upon reductive elimination of H_2 (remember that H_2 evolution was detected during the reaction), the $[(triphos)RhH_2]^+$ system forms, which couples with an identical moiety to give **2** (Scheme III).

In a similar way, when **1** is refluxed in THF, the evolution of H_2 is reasonably followed by the formation of the fragment [(triphos)RhH], which is not stable per se and therefore couples with an intact molecule of **1** forming the neutral dimeric complex **3** (Scheme IV).

It has not been possible to precisely determine the amount of H_2 formed because of the drastic reactions conditions. However, when **1** was heated in THF in the presence of 3,3-dimethylbut-1-ene, **2** was quantitatively obtained together with alkane in a 1:0.5 ratio, thus indicating that only half of **1** transfers hydrogen to the alkene (Scheme V). In other words, coupling of the [(triphos)RhH] moiety with intact **1** appears faster than both the thermal decomposition of **1** and the hydrogen transfer reaction to the alkene.

Conclusive evidence for the intermediacy of the coordinatively and electronically unsaturated fragment $[(triphos)RhH_2]^+$ in the formation of **2** is provided by protonation of **1** in THF by $HOSO_3CF_3$ without being followed by $NaBPh_4$ addition. In fact, in this case no dimeric species is observed. In particular, when the protonation reaction of **1** is carried out an in NMR tube, the $^{31}P\{^1H\}$ NMR spectrum (THF, 303 K) shows an AM_2X spin system 52 ppm, dt, J_{PRh} = 118 Hz, J_{PP} = 30 Hz; 8 ppm, dd, J_{PRh} = 88 Hz), which is typical of $[(triphos)RhH_2(solvent)]^+$.[15] We therefore conclude that the driving force that controls the formation of the binuclear complexes **2** is the addition of the bulky BPh_4^- counteranion.

Once formed, the compound maintains the dimeric structure also in solution. However on long standing in DMF solutions **2** decomposes to yield the $\mu\text{-}H_3$ complex $[(triphos)Rh(\mu\text{-}H)_3Rh(triphos)]BPh_4$ (**4**)[7,6c] (Scheme VI). It takes ca. 12 h to convert 1 g of **2** into 0.85 g of **4**.

We note that this process, which, in practice, corresponds to the elimination of a proton from **2**, is greatly accelerated by the presence of a base such as a tertiary phosphine whereas it is prevented in the presence of strong protic acids. The **2** → **4** transformation is, to certain extent, reversible because the reaction of **4** in THF with $LiHBEt_3$ gives **3**, which is oxidized by atmospheric oxygen to restore **2** (see Scheme VI).

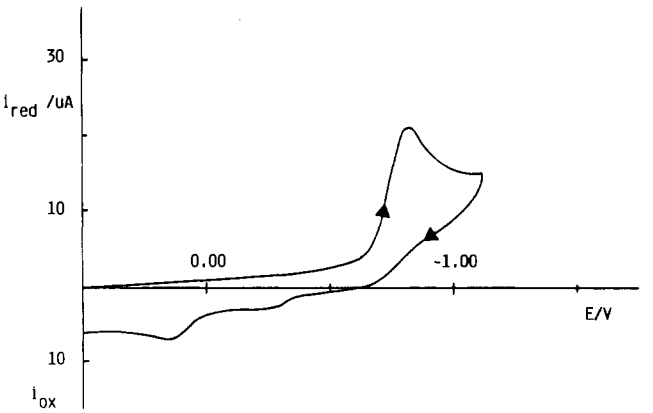

Figure 5. Cyclic voltammogram recorded at a platinum electrode on a DMF solution containing **6** (6.6×10^{-4} mol dm^{-3}) and $[NEt_4]ClO_4$ (0.1 mol dm^{-3}). Scan rate: 0.2 V s^{-1}.

Scheme VI

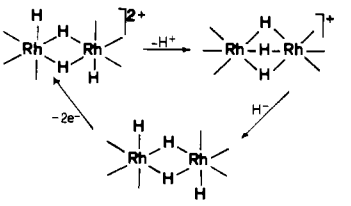

Scheme VII

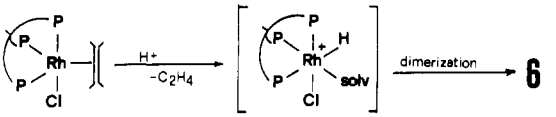

Dichloro-Bridged Complexes. While the formation of **6** by protonation of **5** can be easily interpreted in terms of an oxidative addition/dimerization pathway (Scheme VII), the alternative route involving dissolution of **2** in CH_2Cl_2 apparently proceeds via a double H/Cl exchange: the terminal hydride ligands of **2** after exchanging with chlorine atoms from CH_2Cl_2 intramolecularly exchange with the bridging hydrides. In this respect, one must remember that the preference for bridging chlorides over bridging hydrides in mixed chloride–hydride binuclear complexes is a well-known process, which is generally governed by electronic factors, i.e. the formation of a three-center–four-electron system is preferred over a three-center–two-electron interaction.[8e,16] However, given the larger Cl vs H size, steric factors cannot be completely ruled out.

The presence of chlorine bridges in a complex framework which is essentially that of the all-hydride congener **2** has an enormous influence on both the solution behavior (remember the high fluxionality of **2**) and the redox properties of the molecule. In fact, replacing the bridging hydrides by chlorides makes the compound unable to reversibly accept or lose electrons as shown in Figure 5, which illustrates a cyclic voltammogram of **6** in DMF solution.

A single reduction peak (E_p = −0.84 V) appears in the useful potential range of the solvent. Controlled-potential coulometry at −1.4 V indicated the process to involve a single-step two-electron reduction. The complete electrochemical irreversibility of this process is pointed out by the lack of any directly associated re-

(16) (a) Summerville, R. H.; Hoffmann, R. *J. Am. Chem. Soc.* **1979**, *101*, 3821. (b) Shaik, S.; Hoffmann, R.; Fisel, C. R.; Summerville, R. H. *Ibid.* **1980**, *102*, 4555. (c) Mason, R.; Mingos, D. P. M. *J. Organomet. Chem.* **1973**, *50*, 53.

Scheme VIII

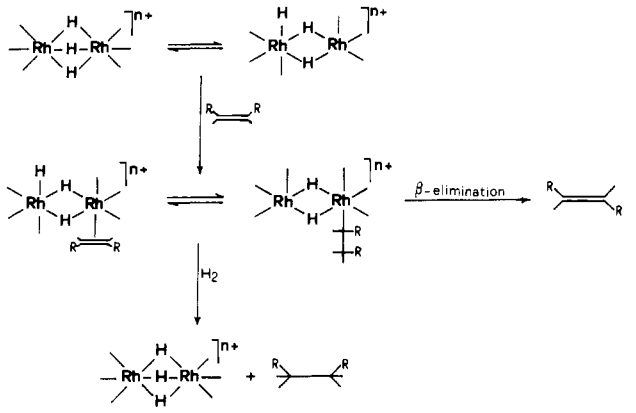

oxidation peak in the reverse scan even at the highest scan rate of 50 V s^{-1}. On the other hand, the presence of a few minor peaks at very anodic potentials in the reverse scan clearly indicates chemical irreversibility, i.e. the occurrence of fast fragmentation reactions following the electron transfer.

Hydrogen-Transfer Reactions. A detailed mechanistic investigation of the catalytic cycles relative to the hydrogenation reactions of DMAD and DMMA by the present family of dimeric rhodium polyhydrides is beyond the purpose of this paper. We wish to stress that we were just interested in comparing and contrasting the hydrogenation reactions of homo- and heterobimetallic polyhydrides in which type and number of the hydride ligands, overall electron count, and the nature of the metals are varied as systematically as possible. In effect, the present family of rhodium polyhydrides presents a unique opportunity to correlate the electronic and geometric structure with catalysis.

Preliminary studies indicate that the compounds generally maintain the dimeric structure during the catalytic cycles. This is a fact that can also be indirectly deduced by the different hydrogenation rates of the mononuclear species as well as the lower activity of the mixed-metal derivative vs homonuclear congeners. In particular, the end products of the reactions with the homodinuclear derivatives **9** and **10** are alkane and the starting metal complexes. In the light of the excellent studies reported by the Muetterties' group on the catalytic hydrogenation of alkenes and alkynes by a family of dirhodium tetrahydrides,[5d,f] we can reasonably propose the sequence shown in Scheme VIII to account for the reactions of **9** and **10**. This involves H_2 oxidative addition to one rhodium atom and olefin coordination to the other rhodium.

At the end of catalytic experiments carried out with appreciable amounts of the mononuclear complexes **7** and **8**, the reaction mixtures separated, after the addition of *n*-butanol, orange crystals that were authenticated by spectroscopic and electrochemical methods as mixtures of **2** and **4**. These results are reasonable since, in both cases, the hydrogenation catalyst is believed to be the 14-electron fragment $[(triphos)Rh]^+$ that is appropriate to oxidatively add H_2 forming $[(triphos)Rh(H)_2]^+$. Ultimately, the latter species dimerizes to **2**, which, in turn, is known to slowly transform to the μ-H_3 complex **4**. In view of these results, one may argue that some of the dirhodium complexes may convert to the mononuclear species under catalytic conditions (added olefin). In this eventuality, the rate differences reported in Tables I and II could be due to induction periods. We are inclined to exclude this hypothesis not only because the turnover rate is higher for the mononuclear species but also because neither **2** nor **4** react with excess of DMAD (or DMMA) to form **7** (or **8**).

Experimental Section

General Information. All reactions and manipulations were routinely performed under a nitrogen atmosphere. Reagent grade chemicals were used in the preparations of the complexes. The solid complexes were collected on a sintered-glass frit and, unless stated otherwise, washed first with ethanol and then with *n*-pentane before being dried in a stream of nitrogen. The compounds $(triphos)RhH_3$ (**1**),[9] and $[(triphos)Rh(\mu\text{-}H)_3Rh(triphos)]BPh_4$ (**4**)[6c,7] were prepared according to published procedures.

Physical Measurements. Infrared spectra were recorded with a Perkin-Elmer 475 grating spectrophotometer or samples mulled in Nujol between KBr plates. ^1H and $^{31}P\{^1H\}$ NMR spectra were taken with a Varian VXR 300 spectrometer. Peak positions are relative to tetramethylsilane and phosphoric acid, respectively, with downfield values reported as positive. Conductance measurements were made with a WTW Model LBR/B conductivity bridge. The materials and the apparatus used for the electrochemical experiments have been described elsewhere.[17] The potential value are relative to an aqueous calomel electrode (SCE). The temperature was controlled at 20 ± 0 °C. Under the present experimental conditions, the ferrocenium/ferrocene couple was located at +0.38 V (MeCN) and at +0.45 V (DMF). X-band EPR spectra were recorded with an ER 200-SRCB Bruker spectrometer operating at w° = 9.78 GHz. The control of the external magnetic field was obtained with a microwave bridge ER 041 MR Bruker wavemeter. The temperature was varied and controlled with an ER 4111 VT Bruker device with an accuracy of ±1 K. To estimate accurate g_{iso} and g_{aniso} values over the temperature range of interest, the diphenylpicrylhydrazyl (DPPH) free radical was used as a field marker (g_{iso} DPPH = 2.0036, w° = 9.43 GHz). To assure quantitative reproducibility, the samples were placed into calibrated quartz capillary tubes permanently positioned in the resonance cavity.

GC analyses were performed on a Shimadzu GC-8A gas chromatograph fitted with a thermal conductivity detector and a 6-ft 0.1% SP-1000 on Carbopack C $^1/_8$-in stainless-steel column (Supelco Inc.). Quantification was achieved with a Shimadzu C-R6A Chromatopac coupled with the chromatograph, operating with an automatic correct area normalization method.

Catalytic Runs. In a typical hydrogenation reaction the substrate (0.9 mmol), DMF (5 mL) and a stirring bar were placed in a reaction vessel fitted with a sidearm with a rubber septum under anaerobic conditions. It was then placed at 1 atm of hydrogen pressure, immersed in a constant-temperature oil bath at 25 or 80 °C, and stirred for 10 min to allow equilibration. The catalyst (0.03 mmol of metal atoms) was added. The solution was sampled at regular intervals by using a 1-μL GC syringe via the rubber septum and the samples were analyzed with a gas chromatograph.

$[(triphos)RhH(\mu\text{-}H)_2HRh(triphos)](BPh_4)_2$ (2). Addition of neat HSO_3CF_3 (45 μL, 0.5 mmol) to **1** (0.36 g, 0.5 mmol) in CH_2Cl_2 (or THF) (25 mL) caused an immediate color change from yellow to red accompanied by H_2 evolution. $NaBPh_4$ (0.17 g, 0.5 mmol) in ethanol (20 mL) was then added, and within a few minutes orange crystals began to precipitate. Further addition of ethanol (5 × 5 mL) completed the precipitation in 20 min; yield 66%. Anal. Calcd for $C_{130}H_{122}B_2P_6Rh_2$: C, 74.43; H, 5.86; Rh, 9.81. Found: C, 73.89; H, 5.71; Rh, 9.73. Λ_M (10^{-3} M nitroethane): 106 $cm^2\ \Omega^{-1}\ mol^{-1}$.

$[(triphos)RhH(\mu\text{-}H)_2HRh(triphos)]$ (3). Method A. A suspension of **1** (0.36 g, 0.5 mmol) in THF (40 mL) was heated at reflux temperature for 30 min during which occurred the concomitant dissolution of the solid and the precipitation of liver red crystals. The mixture was cooled to room temperature and the crystals were collected by filtration and washed with a 3:1 mixture of *n*-pentane/THF; yield 91%. When the reaction was carried out in the presence of an excess of 3,3-dimethylbut-1-ene, GC analysis of the liquid phase revealed the formation of 2,2-dimethylbutane with a stoichiometry of 0.5 mol/mol of 1. Anal. Calcd for $C_{82}H_{82}P_6Rh_2$: C, 67.54; H, 5.66; Rh, 14.11. Found: C, 67.58; H, 5.57; Rh, 14.07.

Method B. Addition of $LiHBEt_3$ (1 M in THF) (0.3 mL) to a suspension of **4** (0.37 g, 0.2 mmol) in THF (15 mL) caused the solid to dissolve, giving a deep red solution. Few drops of ethanol were added, and within a few minutes liver red crystals precipitated in 87% yield that were filtered off and washed as above.

Reaction of 3 with O_2. A mixture of **3** (0.29 g, 0.2 mmol) and $NaBPh_4$ (0.07 g, 0.2 mmol) in a 1:2 mixture of DMF/THF (10 mL) was stirred in air for 2 h during which the solid slowly dissolved to give a red solution. Addition of *n*-butanol (30 mL), under nitrogen, gave orange crystals of **2**; yield 62%.

$[(triphos)RhH(\mu\text{-}Cl)_2HRh(triphos)](BPh_4)_2$ (6). Neat HSO_3CF_3 (27 μL, 0.3 mmol) was added to a solution of **5** (0.24 g, 0.3 mmol) in CH_2Cl_2 (20 mL). There was an immediate color change from orange to light red. Addition of $NaBPh_4$ (0.17 g, 0.5 mmol) and ethanol (25 mL) led to the precipitation of pink crystals; yield 84%. Anal. Calcd for $C_{130}H_{120}b_2Cl_2P_6Rh_2$: C, 72.06; H, 5.58; Rh, 9.49. Found: C, 71.77; H, 5.49; Rh, 9.39. Λ_M (10^{-3} M nitroethane): 102 $cm^-\ \Omega^{-1}\ mol^{-1}$.

$[(triphos)Rh(\pi\text{-DMAD})]BPh_4$ (7) and $[(triphos)Rh(\pi\text{-DMMA})]BPh_4$ (8). A 3-fold excess of neat DMAD or DMMA was pipetted into a

(17) Bianchini, C.; Mealli, C.; Meli, A.; Sabat, M.; Zanello, P. *J. Am. Chem. Soc.* **1987**, *109*, 185.

CH_2Cl_2 (30 mL) solution of **5** (1 mmol). After the mixture was stirred for 15 min, addition of $NaBPh_4$ (1 mmol) in ethanol (30 mL), followed by slow concentration, gave red orange or yellow crystals, respectively, in ca. 85% yield. Full physical-chemical characterization of both complexes will be published elsewhere.[14] We anticipate here that **8** has an octahedral geometry, the rhodium atom being coordinated by the three phosphorus atoms of triphos, the two carbon atoms of the olefin, and one of the two ester carbonyl double bonds. In contrast, **7** is five-coordinated by the three phosphorus atoms of triphos and the alkyne molecule, which acts as a 4e donor.

Acknowledgment. We are indebted to the Conselleria de Educacion de la Generalitat Valenciana for a grant that made J.A.R.'s stay at Florence possible.

Registry No. **1**, 100333-94-6; **2**, 105736-81-0; **3**, 116863-68-4; **4**, 104103-47-1; **5**, 105139-41-1; *trans*-**6**, 116863-70-8; *cis*-**6**, 116946-97-5; **7**, 116863-74-2; **8**, 116863-72-0; **9**, 104103-48-2; **10**, 104103-50-6; **11**, 104119-29-1; DMAD, 762-42-5; DMMA, 624-48-6; DMFU, 624-49-7; DMSU, 106-65-0; [(triphos)RhH(μ-H)$_2$HRh(triphos)]$^+$, 116887-36-6; 3,3-dimethylbut-1-ene, 558-37-2.

Contribution from the Department of Chemistry, University of Queensland, Brisbane, Australia 4067

^{15}N NMR Spectra of Pentaamminerhodium(III) Complexes

Trevor G. Appleton, John R. Hall,* and Stephen F. Ralph

Received December 23, 1987

A series of pentaamminerhodium(III) complexes, $Rh(NH_3)_5Z^{n+}$, has been prepared, with 80% enrichment in ^{15}N (Z = H_2O, OH^-, Cl^-, Br^-, I^-, NH_3, $-ONO^-$, $-NO_2^-$, $-NCS^-$, $-SCN^-$, $-NCO^-$, CN^-). The ^{1}H-decoupled ^{15}N NMR spectra show two doublets (from coupling to ^{103}Rh) with approximate intensity ratio 4:1. δ_N and ^1J(Rh-N) are sensitive to Z, especially for the unique ammine trans to Z. Good correlations exist between δ_N in this series and δ_N in the corresponding cobalt(III) complexes $Co(NH_3)_5Z^{n+}$ and platinum(II) complexes $Pt(NH_3)_3Z^{m+}$. J(Rh-N) trans to Z also correlates well with J(Pt-N) trans to Z in the platinum series.

Introduction

^{15}N NMR has been used extensively to study reactions in solution of ammineplatinum complexes.[1-7] To help place the interpretation of ^{15}N NMR parameters on a firm empirical basis, we have carried out a systematic study of the effect of Z on these parameters in the series of triammineplatinum(II) complexes $Pt(NH_3)_3Z^{m+}$ (**1**) and meridional triammineplatinum(IV) complexes $Pt(NH_3)_3Z(OH)_2^{m+}$ (**2**).[8] With these series the influence

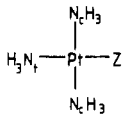

1

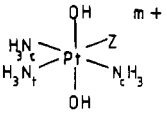

2

of Z on the ammine ligands trans and cis to Z could be studied simultaneously. The usefulness of ^{15}N NMR in ammineplatinum systems arises from the following properties: (i) Each distinct ammine ligand gives a separate sharp signal. (ii) δ_N and the coupling constant between ^{15}N and the metal nucleus both depend in a predictable way on the ligands cis and trans to ammine (especially trans). (iii) The spectrum is not complicated by coupling between nonequivalent ^{15}N nuclei from ammine ligands cis to each other.

Despite the successful application of ^{15}N NMR spectroscopy with ^{15}N-enriched ammine ligands to the chemistry of ammine complexes of platinum, we are not aware of any attempts to apply this technique to the study of ammine complexes of other metals. To assess its potential in the investigation of the chemistry of ammine complexes of rhodium(III), we have now prepared a series of pentaamminerhodium(III) complexes, $Rh(NH_3)_5Z^{n+}$ (**3**), in

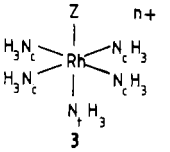

3

which there is 80% enrichment of the ammine ligands with ^{15}N ($I = {}^1/_2$), and obtained their ^{15}N NMR spectra. The only naturally occurring isotope of rhodium is ^{103}Rh ($I = {}^1/_2$). We are aware of only one report on the ^{14}N chemical shift of $Rh(NH_3)_6^{3+}$.[9] Nitrogen shifts are now available for a number of pentaamminecobalt(III) complexes,[10] and it is of interest to compare trends for the rhodium complexes with those in that series.

Table I. ^{15}N NMR Data for Pentaamminerhodium(III) Complexes $Rh(NH_3)_5Z^{n+}$ (**3**)

Z	NH_3 trans to Z (N_t)		NH_3 cis to Z (N_c)	
	δ_{N_t}	J(Rh-N_t), Hz	δ_{N_c}	J(Rh-N_c), Hz
H_2O	-77.33	17.3	-57.81	13.9
OH^-	-68.54	13.9	-57.46	14.2
Cl^-	-66.14	15.4	-57.93	13.4
Br^-	-60.53	14.9	-59.84	13.4
I^-	-50.02	13.4	-63.17	13.4
NH_3	-59.83	14.2	-59.83	14.2
$-ONO^-$	-73.24	15.1	-56.31	14.2
$-NO_2^-$	-60.41	12.2	-52.91	14.4
$-NCS^-$	-66.45	16.1	-59.26	13.7
$-SCN^-$	-52.42	13.7	-58.08	13.7
$-NCO^-$	-67.28	15.1	-58.86	13.2
CN^-	-42.32	10.3	-62.66	13.2

(1) Alei, M.; Vergamini, P. J.; Wageman, W. E. *J. Am. Chem. Soc.* **1979**, *101*, 5415.
(2) Boreham, C. J.; Broomhead, J. A.; Fairlie, D. P. *Aust. J. Chem.* **1981**, *34*, 659.
(3) Chikuma, M.; Pollock, R. J. *J. Magn. Reson.* **1982**, *47*, 324.
(4) Nee, M.; Roberts, J. D. *Biochemistry* **1982**, *21*, 4920.
(5) Ismail, I. M.; Sadler, P. J. *In Platinum, Gold, and Other Metal Chemotherapeutic Agents*; Lippard, S. J., Ed.; American Chemical Society: Washington, DC, 1983; p 171.
(6) Appleton, T. G.; Berry, R. D.; Davis, C. A.; Hall, J. R.; Kimlin, H. A. *Inorg. Chem.* **1984**, *23*, 3514.
(7) Appleton, T. G.; Hall, J. R.; Ralph, S. F. *Aust. J. Chem.* **1986**, *39*, 1347.
(8) Appleton, T. G.; Hall, J. R.; Ralph, S. F. *Inorg. Chem.* **1985**, *24*, 4685.
(9) Bramley, R.; Figgis, B. N.; Nyholm, R. S. *J. Chem. Soc. A* **1967**, 861.
(10) Bramley, R.; Brorsen, M.; Sargeson, A. M.; Schaffer, C. E. *Inorg. Chem.* **1987**, *26*, 314.

0020-1669/88/1327-4435$01.50/0